Biogeosciences Discuss., 12, 15111–15156, 2015
www.biogeosciences-discuss.net/12/15111/2015/
doi:10.5194/bgd-12-15111-2015

Biogeosciences
Discussions
Open Access

Sedimentological processes and environmental variability at Lake Ohrid (Macedonia, Albania) between 640 ka and present day

A. Francke[1], **B. Wagner**[1], **J. Just**[1], **N. Leicher**[1], **R. Gromig**[1], **H. Baumgarten**[2], **H. Vogel**[3], **J. H. Lacey**[4,5], **L. Sadori**[6], **T. Wonik**[2], **M. J. Leng**[4,5], **G. Zanchetta**[7], **R. Sulpizio**[8,9], **and B. Giaccio**[10]

[1]Institute for Geology and Mineralogy, University of Cologne, Cologne, Germany
[2]Leibniz Institute for Applied Geophysics (LIAG), Hannover, Germany
[3]Institute of Geological Sciences and Oeschger Centre for Climate Change Research, University of Bern, Bern, Switzerland
[4]Centre for Environmental Geochemistry, School of Geography, University of Nottingham, Nottingham, UK
[5]NERC Isotope Geosciences Facilities, British Geological Survey, Keyworth, Nottingham, UK
[6]Dipartimento di Biologia Ambientale, Università di Roma "La Sapienza", Rome, Italy
[7]Dipartimento di Scienze della Terra, University of Pisa, Pisa, Italy
[8]Dipartimento di Scienze della Terra e Geoambientali, University of Bari, Bari, Italy

[9]Istituto per la Dinamica dei Processi Ambientali (IDPA) CNR, Milan, Italy
[10]Istituto di Geologia Ambientale e Geoingegneria – CNR, Rome, Italy

Received: 13 August 2015 – Accepted: 25 August 2015 – Published: 11 September 2015

Correspondence to: A. Francke (alexander.francke@uni-koeln.de)

Published by Copernicus Publications on behalf of the European Geosciences Union.

Abstract

Lake Ohrid (FYROM, Albania) is thought to be more than 1.2 million years old and hosts more than 200 endemic species. As a target of the International Continental Scientific Drilling Program (ICDP), a successful deep drilling campaign was carried out within the scope of the Scientific Collaboration on Past Speciation Conditions in Lake Ohrid (SCOPSCO) project in 2013. Here, we present lithological, sedimentological, and (bio-)geochemical data from the upper 247.8 m of the overall 569 m long DEEP site sediment succession from the central part of the lake. According to an age model, which is based on nine tephra layers (1st order tie points), and on tuning of biogeochemical proxy data to orbital parameters (2nd order tie points) and to the global benthic isotope stack LR04 (3rd order tie points), respectively, the analyzed sediment sequence covers the last 640 ka.

The DEEP site sediment succession consists of hemipelagic sediments, which are interspersed by several tephra layers and infrequent, thin (< 5 cm) mass wasting deposits. The hemipelagic sediments can be classified into three different lithotypes. Lithotype 1 and 2 deposits comprise calcareous and slightly calcareous silty clay and are predominantly attributed to interglacial periods with high primary productivity in the lake during summer and reduced mixing during winter. The data suggest that high ion and nutrient concentrations in the lake water promoted calcite precipitation and diatom growth in the epilmnion in during MIS15, 13, and 5. Following a strong primary productivity, highest interglacial temperatures can be reported for MIS11 and 5, whereas MIS15, 13, 9, and 7 were comparable cooler. Lithotype 3 deposits consist of clastic, silty clayey material and predominantly represent glacial periods with low primary productivity during summer and longer and intensified mixing during winter. The data imply that most severe glacial conditions at Lake Ohrid persisted during MIS16, 12, 10, and 6 whereas somewhat warmer temperatures can be inferred for MIS14, 8, 4, and 3. Interglacial-like conditions occurred during parts of MIS14, and 8.

BGD
12, 15111–15156, 2015

1 Introduction

Long sediment successions from lacustrine basins have been shown to provide valuable archives of local environmental variability and of global climate change during the Quaternary and Neogene (Prokopenko et al., 2006; Melles et al., 2012; Stockhecke et al., 2014a). As lakes are highly sensitive to environmental change (e.g. Cohen, 2003), these lacustrine paleoclimate records commonly document external forcing mechanism via internal feedback processes in their sedimentological records. External forcing mechanisms are the global glacial/interglacial climatic variability, which characterize climate conditions during the Quaternary (EPICA-members, 2004; NGRIP-members, 2004; Lisiecki and Raymo, 2005; Raymo et al., 2006). Additional external forcing mechanisms comprise orbital parameters and the effects of the local insolation on the terrestrial realm. Lake basins thus have the potential to provide high-resolution, continuous paleo-records of global climate change and its impact on regional environments.

Long terrestrial paleo-records in the eastern and southeastern Mediterranean region have become available from Lake Van (Stockhecke et al., 2014b) and from the Dead Sea (Stein et al., 2011). In the central Mediterranean Region, the only terrestrial paleo-records that continuously covers more than one million year is the Tenaghi Philippon pollen record in northern Greece (cf. Fig. 1), which spans the last 1.3 million years and provides fundamental insights into the vegetation history of the area (e.g. Tzedakis et al., 2006). However, analytical methods for paleoclimate reconstructions have so far been restricted to pollen analyses and the sensitivity of vegetation changes to short-term climate variability can be low (e.g. Panagiotopoulos et al., 2013).

Lake Ohrid on the Balkan Peninsula is thought to be more than 1.2 million years old and has already demonstrated its high sensitivity to environmental change and the potential to provide high-resolution paleoenvironmental information for the last glacial/interglacial cycle (e.g. Wagner et al., 2008, 2009, 2014; Vogel et al., 2010a). Given that Lake Ohrid is also a hotspot for endemism with more than 200 endemic

BGD
12, 15111–15156, 2015
Sedimentological processes and environmental variability at Lake Ohrid
A. Francke et al.

species in the lake (Albrecht and Wilke, 2009), its sediment records also have the potential to address evolutionary questions such as what the main triggers of speciation events are.

Based on up to 15 m long sediment cores, which were recovered between 2003 and 2011 (e.g. Wagner et al., 2009, 2012; Vogel et al., 2010a), and on hydro-acoustic surveys carried out between 2004 and 2008 (e.g. Lindhorst et al., 2010), the Scientific Collaboration on Past Speciation Conditions in Lake Ohrid (SCOPSCO) project was established within the scope of the International Continental Scientific Drilling Program (ICDP). The main objectives of the SCOPSCO project are (1) to reveal the precise age and origin of Lake Ohrid, (2) to unravel the seismotectonic history of the lake area including effects of major earthquakes and associated mass wasting events, (3) to obtain a continuous record containing information on volcanic activities and climate changes in the central northern Mediterranean region, and (4) to better understand the impact of major geological/environmental events on general evolutionary patterns and shaping an extraordinary degree of endemic biodiversity as a matter of global significance.

The ICDP deep drilling campaign took place in spring 2013 using the Deep Lake Drilling System (DLDS) operated by the Drilling, Observation and Sampling of the Earths Continental Crust (DOSECC) consortium. More than 2100 m of sediments were recovered from four different drill sites. The processing of the cores from the DEEP site in central part of Lake Ohrid (Fig. 1) is still ongoing at the University of Cologne (Germany). Here, we present lithological, sedimentological, and (bio-)geochemical results from the upper part of the DEEP site sediment succession, which covers the period since 640 ka.

2 Site information

Lake Ohrid is located at the border of the Former Yugoslav Republic of Macedonia (FYROM) and Albania at an altitude of 693 m a.s.l. (above sea level, Fig. 1a). The lake

BGD
12, 15111–15156, 2015

is approximately 30 km long and 15 km wide and covers a surface area of 358 km^2. Due to its location in a tectonic, N–S trending graben system, the bathymetry is tub-shaped with a mean water depth of 150 m and a maximum water depth of 293 m (Fig. 1b). The water volume calculates to 55.4 km^3. The lake is mainly fed by karstic inflow (55 %, e.g. Matzinger et al., 2007; Vogel et al., 2010a; cf. Fig. 1), and by small rivers. The karstic inflow partly originates from Lake Prespa, located at an altitude of 848 m a.s.l. ca. 10 km to the east of Lake Ohrid (Fig. 1b). Both lakes are connected via karstic aquifers. The lake level of Ohrid is balanced by a surface outflow in the northern corner (Crim Drim River, 60 %, Fig. 1b), and by evaporation (40 %, Matzinger et al., 2006a). The large water volume and the high proportion of karstic inflow induce an oligotrophic state of Lake Ohrid. A complete overturn of the water column occurs approximately every 7 years (e.g. Matzinger et al., 2007). The upper about 200 m of the water column are mixed every year.

The catchment of Lake Ohrid comprises 2393 km^2 including Lake Prespa (Fig. 1b). Both lakes are separated by the up to 2300 m a.s.l. high Galicia mountain range (Fig. 1b). To the west of Lake Ohrid, the Mocra mountain chain reaches up to about 1500 m a.s.l. The morphostructure with high mountains to the west and east of Lake Ohrid is mainly the result of a pull-apart like opening of the basin during the late phases of the Alpine orogeny (Aliaj et al., 2001; Hoffmann et al., 2010). Several earthquakes in the area (NEIC database, USGS) and mass wasting deposits, which occur in the lateral parts of Lake Ohrid (Reicherter et al., 2011; Lindhorst et al., 2012; Wagner et al., 2012), document the tectonic activity in the area until present day.

The oldest bedrock in the catchment of Lake Ohrid is of Devonian age, consists of metasediments (phyllites), and occurs in the northeastern part of the basin. Triassic carbonates and siliciclastics occur in the southeast, east, and northwest (e.g. Wagner et al., 2009; Hoffmann et al., 2010; Vogel et al., 2010b). Ultramafic metamorphic and magmatic rocks including ophiolites of Jurassic and Cretaceous age crop out in the west (Hoffmann et al., 2010). Quaternary lacustrine and fluvial deposits cover the plains to the north and to the south of Lake Ohrid (Hoffmann et al., 2010; Vogel et al., 2010b).

The climate at Lake Ohrid is influenced both by continental and Mediterranean climate conditions (Watzin et al., 2002). Between summer and winter, monthly average air temperatures range between 26 and −1 °C, respectively. The annual precipitation averages to ca. 750 mm yr^{1}, with drier conditions during summer, and more precipitation during winter. The prevailing wind directions are north and south and are controlled by the topography of the Lake Ohrid valley (summarized by Wagner et al., 2009).

3 Material and methods

3.1 Field work

The DEEP site (5045-1) is the main drill site in the central part of the lake (Fig. 1b, 41°02′57′′ N, 20°42′54′′ E). The uppermost sediments at the DEEP site down to 1.5 m b.l.f. (below lake floor) were recovered in 2011 using a UWITEC gravity and piston corer (core Co1261), as these drilling techniques provide a good core quality for sub-surface sediments. In 2013, more than 1500 m of sediments were recovered from six different drill holes (5045-1A to 5045-1F) at the DEEP site. The distance between each drill hole averages ca. 40 m. Holes 5045-1A and 5045-1E comprise surface sediments down to ca. 2.4 and 5 m b.l.f., respectively. Holes 5045-1B and 5045-1C were drilled down to a penetration depth of 480 m b.l.f. At hole 5045-1D, the maximum penetration of 569 m b.l.f. was reached. Spot coring down to 550 m b.l.f. was conducted in hole 5045-1F in order to fill gaps of the other holes (see also Wagner et al., 2014). After core recovery, the sediment cores were cut into up to one meter long segments and stored in darkness at 4 °C.

During the drilling campaign in 2013, onsite core processing comprised smear-slide analyses of core catcher material and magnetic susceptibility measurements on the whole cores in 2 cm resolution using a Multi-Sensor Core Logger (MSCL, GEOTEK Co.) and a Bartington MS2C loop sensor (see also Wagner et al., 2014). Following

BGD
12, 15111–15156, 2015

Title Page
Abstract | Introduction
Conclusions | References
Tables | Figures
◂◂ | ▸▸
◂ | ▸
Back | Close
Full Screen / Esc
Printer-friendly Version
Interactive Discussion

the field campaign, the cores were shipped to the University of Cologne for further analyses.

3.2 Laboratory work

A first correlation of the individual core segments to provide a preliminary composite profile for the DEEP site sequence was established based on the magnetic susceptibility data of the whole cores from holes 5045-1B, 5045-1C, 5045-1D, and 5045-1F. Cores included into the composite profile were then split lengthwise and described for color, grain-size, structure, macroscopic components, and calcite content (reaction with 10 % HCl). High-resolution line scan images were taken using the MSCL (GEOTEK Co.). X-ray Fluorescence (XRF) scanning was carried out at 2.5 mm resolution and with an integration time of 10 s using an ITRAX core scanner (Cox Analytical, Sweden). The ITRAX core scanner was equipped with a chromium (Cr) X-Ray source and was run at 30 kV and 30 mA. Data processing was performed with the software QSpec 6.5 (Cox Analytical, Sweden, cf. Wennrich et al., 2014). In order to account for inaccuracies and to validate the quality of the XRF- scanning data, conventional wavelength dispersive XRF (WDXRF, Philips PW 2400, Panalytical Cor., the Netherlands) was conducted at 2.56 m resolution. The optical and lithological information (layer by layer correlation) were then combined with XRF scanning data for a fine tuning of the core correlation by using the Corewall software package (Correlator 1.695 and Corelyzer 2.0.1).

If an unequivocal core correlation was not possible, additional core sections from other drill holes in the respective depths were opened, likewise analyzed, and used for a refinement of the core correlation. In the composite profile, the field depth measurements based on “meters below lake floor” (m b.l.f.) were replaced by “meters composite depth” (m c.d.). The DEEP site composite profile down to 247.8 m c.d. comprises two sections of core Co1261 for the uppermost 0.93 m c.d. and in total 386 core sections from holes 5045-1B, 5045-1C, 5045-1D, and 5045-1F (Fig. 2, Table 1). The overall recovery of the composite profile calculates to 99.97 %, as no overlapping sequences were found between core run numbers 80 and 81 in hole 5045-1C. The length of the core catcher (8.5 cm) between these two runs led to one gap between 204.719 and 204.804 m c.d.

At 16 cm resolution, 2 cm thick slices (40.7 cm^3) were removed from the core half and separated into four sub-samples to establish a multiproxy data set. Intermediate intervals (8 cm distance to the 2 cm thick slices) were subsampled for high-resolution studies by pushing two cylindrical plastic vials (diameter = 0.9 cm, height = 4 cm, volume = 2.5 cm^3) into the core halves. In addition, samples for paleomagnetic analyses were taken in cubic plastic boxes (volume of 6.2 cm^3) at 50 cm resolution until 100 m c.d., and at 48 cm resolution below this depth (cf. Just et al., 2015).

All sub-samples (8 cm resolution) were freeze-dried, and the water content was calculated by the difference in weight before and after drying. For every other sample, an aliquot of about 100 mg was homogenized and ground to < 63 µm. For the measurement of total carbon (TC) and total inorganic carbon (TIC) using a DIMATOC 100 carbon analyzer (Dimatec Corp., Germany), 40 mg of this aliquot was dispersed with an ultrasonic disperser in 10 mL DI water. TC was measured as released CO_2 after combustion at 900 °C. The TIC content was determined as CO_2 after treating the dispersed material with phosphoric acid (H_3PO_4) and combustion at 160 °C. The total organic carbon (TOC) content was calculated from the difference between TC and TIC. For the measurement of total sulfur (TS) and total nitrogen (TN), 10 mg of the ground material was analyzed using an elemental analyzer (vario cube, elementar Corp.) after combustion at 1150 °C.

Biogenic silica (bSi) concentrations were determined at 32 cm resolution by means of Fourier Transform Infrared Spectroscopy (FTIRS) at the Institute of Geological Sciences, University of Bern, Switzerland. For sample preparation, 0.011 g of each sample was mixed with 0.5 g of oven-dried spectroscopic grade potassium bromide (KBr) (Uvasol®, Merck Corp.) and subsequently homogenized using a mortar and pestle. A Bruker Vertex 70 equipped with a DTGS (Deuterated Triglycine Sulfate) detector, a KBr beam splitter, and a HTS-XT accessory unit (multi-sampler) was used for the measurement. Each sample was scanned 64 times at a resolution of 4 cm^{-1} (recipro-

BGD
12, 15111–15156, 2015

cal centimeters) for the wavenumber range from 3750 to 450 cm^{-1} in diffuse reflectance mode. After the measurements, linear baseline correction was applied to normalize the recorded FTIR spectra and to remove baseline shifts and tilts by setting two points of the recorded spectrum to zero (3750 and 2210–2200 cm^{-1}). The determination of bSi from FTIR spectral information relies on spectral variations in synthetic sediment mixtures with known bSi concentrations and calibration models between the FTIR spectral information and the corresponding bSi concentrations based on partial least squares regression (PLSR, Wold et al., 2001 and references therein). For details and information regarding groundtruthing of the calibration see Meyer-Jacob et al. (2014).

For grain-size analyses at 64 cm resolution, 1.5 g of the sample material was treated with hydrogen peroxide (H_2O_2, 30 %), hydrochloric acid (HCl, 10 %), sodium hydroxide (NaOH, 1 M), and $Na_4P_2O_7$. Prior to the analyses, the sample material was dispersed on a shaker for 12 h and underwent one minute of ultrasonic treatment. Sample aliquots were then measured three times with a Saturn DigiSizer 5200 laser particle analyzer equipped with a Master Tech 52 multisampler (Micromeritics Co., USA) and the individual results were averaged. Data processing was carried out by using the GRADISTATv8 program (Blott and Pye, 2001).

4 Results and discussion

4.1 Lithology

The sediments from the DEEP site sequence down to 247.8 m c.d. consist of fine-grained hemipelagic sediments, which are sporadically interspersed by more coarse-grained event layers. From the top to the bottom, the water content decreases from a maximum of 70 % to a minimum of 32 % due to compaction by overlying deposits (for detailed studies on the sediment compaction at the DEEP site see Baumgarten et al., 2015).

BGD
12, 15111–15156, 2015

4.1.1 Hemipelagic sediments

The hemipelagic deposits of the DEEP site sequence were subdivided into three lithotypes (Figs. 2 and 3) based on information from the visual core descriptions. This includes variations in the calcite content (reaction with 10 % HCl), and the sediment color and structure.

The sediments of *lithotype 1* (Figs. 2 and 3) show strong to very strong reactions with 10 % HCl, have very dark greenish grey to greenish grey colors, and appear massive, bioturbated, or finely laminated. Silt to gravel-sized vivianite concretions occur irregularly distributed within lithofacies 1 and can be identified by a color change from grey to blue after core opening.

The strong to very strong reaction with 10 % HCl and TIC contents between 2 and 9.7 % imply that calcite ($CaCO_3$) is abundant in lithotype 1 sediments. Changes in color correspond to different calcite and TOC contents in the deposits (Fig. 3). The TOC content can be used as an indicator for the amount of finely dispersed organic matter (OM) in lacustrine deposits (e.g. Cohen, 2003; Stockhecke et al., 2014a). In the sediments of lithotype 1, bright colors (greenish grey) are commonly correlated with massive layers and are indicative for high calcite and low OM contents. Dark (very dark greenish grey, dark greenish grey) lithotype 1 deposits appear bioturbated and have lower calcite and higher OM concentrations. Laminated successions occur only in the upper meter of the DEEP site sequence. The bSi contents in the sediments of lithotype 1 vary between 1.9 and 42.5 % and suggest that diatom frustules can be abundant. Low potassium intensities (K, Fig. 2) correspond to minima in the fine fraction (< 4 µm, Fig. 2) of the grain size classes and imply a low abundance of siliciclastic minerals in lithotype 1 sediments (cf. Arnaud et al., 2005; Wennrich et al., 2014).

Lithotype 2 sediments exhibit a moderate reaction with 10 % HCl, are greenish black and very dark greenish grey in color, and appear bioturbated or massive. Vivianite concretions occur irregularly, and yellowish brown layers yield high amounts of siderite ($FeCO_3$) crystals in smear-slide samples (Figs. 2 and 4).

The moderate reaction with 10 % HCl implies that calcite is less abundant in lithotype 2 sediments, which is consistent with TIC contents between 0.5 and 2 %. Distinct peaks in the TIC content correspond to peaks in Fe and Mn counts and to the occurrence of the yellowish brown siderite layers (Fig. 4). The greenish black sediment successions of lithotype 2 sediments are bioturbated and have high amounts of OM, as indicated by TOC contents of up to 4.5 %. Brighter, very dark greenish grey sections can be massive or bioturbated and have lower TOC contents (Fig. 3). The amount of diatom frustules is moderate to high, as inferred from bSi contents between 2 and 27.9 %, and the amount of clastic matter is moderate (Fig. 2, K-intensities).

The bright, greenish grey sediments of *lithotype 3* do not show a reaction with 10 % HCl, are bioturbated and intercalated with massive sections of up to several decimeters thickness (Fig. 3). Vivianite concretions occur irregularly, and yellowish brown siderite layers are abundant (Fig. 2).

The TIC values of lithotype 3 sediments rarely exceed 0.5 %, which infers negligible calcite contents, and matches the null reaction to 10 % HCl. Peaks in TIC, which occasionally exceed 0.5 % can be attributed to the occurrence of siderite layers (Figs. 2 and 4). TOC ranges between 0.4 and 4.8 % (Fig. 2), with higher values > 2.5 % close to the lower and upper boundaries of lithotype 3 sediment sections, and between 3.21 and 2.89 m c.d. (Fig. 2). The amount of bSi is mostly between 1.68 and 14.5 %, except for several peaks of up to 41.3 % above tephra layers. High potassium intensities throughout most parts of lithotype 3 sediments indicate high clastic matter contents and correspond to high percentages of the fine fraction (< 4 µm, Fig. 2).

4.1.2 Event layers

The macroscopic event layers were classified as tephra deposits if exclusively glass shards were observed in the smear slides, and as mass movement deposits (MMD) if predominantly minerogenic components or a mixture of glass shards from different tephras occurred (cf. Figs. 2 and 3). Tephra layers in the DEEP site sequence appear as up to 15 cm thick layers and as lenses (cf. Leicher et al., 2015). Most of the tephra layers are between 0.5 and 5 cm thick (e.g. Fig. 3, 1D-18H-3, 85 to 82 cm section depth, 1D-6H-2, 23 to 21 cm section depth). Tephrostratigraphic work including geochemical analyses of glass shards enabled the correlation of eight tephra layers from the DEEP site sequence to known volcanic eruptions in the central Mediterranean Region (cf. Table 2, Leicher et al., 2015). In addition, a distinct peak in the K concentration in the DEEP site sequence at 2.773 m c.d. was identified as the Mercato crypto tephra layer (cf. Table 2) by a correlation the K XRF curve to those of cores Co1202 (Sulpizio et al., 2010; Vogel et al., 2010c) and Co1262 (Wagner et al., 2012, for locations of the cores see Fig. 1). In cores Co1202 and Co1262, glass shards that co-occurred with a significant potassium peak were identified as the Mercato crypto tephra layer and glass shards were also found in the DEEP site, where the corresponding K peak was identified.

The MMDs in the DEEP site sequence are between 0.1 and 3 cm thick, and consist of very coarse silt to fine sand-sized material (cf. also Fig. 3). A higher frequency of MMD's occurs between 117 and 107 m c.d., and between 55 and 50 m c.d., respectively. Most of the MMD's appear normal graded (Fig. 3, 1C-68H-2, 70 to 68 cm section depth), or as lenses (Fig. 3, 1D-24H-2, 41 to 39 cm section depth). In some very thin MMDs, the graded structures are only weakly expressed. The MMD in core 1F-4H-3 (Fig. 2, 3, 17 to 14 cm section depth) differs from all other MMDs in the DEEP site sequence as it is the only one with a clay layer at the top, and a 1.5 cm thick, poorly sorted, clay to fine sand-sized section at the bottom. In the overlapping core sections from holes 5045-1B, 5045-1C, and 5045-1D, the basal, poorly sorted part of the MMD in 1F-4H-3 is not preserved.

4.2 Sedimentary processes

4.2.1 Hemipelagic sediments

As shown by Scanning Electron Microscope (SEM) and X-ray Diffraction (XRD) analyses (e.g. Wagner et al., 2009; Leng et al., 2010), the calcite in the sediments of Lake

BGD
12, 15111–15156, 2015

Title Page
Abstract | Introduction
Conclusions | References
Tables | Figures
◀| |▶
◀ ▶
Back | Close
Full Screen / Esc
Printer-friendly Version
Interactive Discussion

Ohrid is mainly endogenic and the amount of detrital carbonates is considered to be negligible despite the high abundance of limestones in the catchment. Only minor contributions to the calcite content come from biogenic sources, for example from ostracod valves (Vogel et al., 2010a). Endogenic calcite deposition in the sediments of Lake Ohrid is predominately triggered by photosynthesis-induced formation of calcite crystals in the epilimnion (e.g. Wagner et al., 2009; Vogel et al., 2010a). The precipitation occurs at warm temperatures during spring and summer, as long Ca^{2+} and HCO^{3-} ions are not short in supply (e.g. Matzinger et al., 2007; Wagner et al., 2009; Vogel et al., 2010a). High Ca^{2+} and HCO^{3-} concentrations in Lake Ohrid are triggered by the intensity of chemical weathering and limestone dissolution in the catchment, the amount of incoming water, and the evaporation of lake water (Vogel et al., 2010a). The calcium carbonate concentration in the sediments also depends on the preservation of the endogenic calcite. Dissolution of calcite at the sediment surface and lower parts of the water column can be caused by oxidation of OM, which triggers H_2CO_3 release from the surface sediments and a lowering of the lake-water pH (Müller et al., 2006; Vogel et al., 2010a). SEM analyses indicate that microbial dissolution of endogenic calcite can be observed in the DEEP site sequence (Lacey et al., 2015).

The high TIC contents in lithotype 1 imply high photosynthesis induced precipitation of endogenic calcite, high temperatures during spring and summer, good calcite preservation in the sediments, and buffering of the lake water pH. Lower primary productivity, lower temperatures and probably at least partly dissolution of calcite can be inferred from the TIC record in lithotype 2 and 3 sediments. In lithotype 2 and 3, siderite layers ($FeCO_3$) also contribute to the TIC content (cf. Figs. 2 and 4). In neighboring Lake Prespa, siderite formation has been reported to occur in the surface sediments close to the redox boundary under acid and reducing conditions (Leng et al., 2013). In Lake Ohrid, DEEP site lithotype 2 and 3 sediments contain discrete horizons of authigenic siderite crystals and crystal clusters nucleating within an unconsolidated clay matrix (Lacey et al., 2015). The open-packed nature of the matrix and growth relationships between crystals suggest that, as also observed in Lake Prespa, siderite formed in

Discussion Paper | Discussion Paper | Discussion Paper | Discussion Paper |

BGD

12, 15111–15156, 2015

Sedimentological processes and environmental variability at Lake Ohrid

A. Francke et al.

Title Page
Abstract Introduction
Conclusions References
Tables Figures
◂◂ ▸▸
◂ ▸
Back Close
Full Screen / Esc
Printer-friendly Version
Interactive Discussion

surface sediments close to the sediment–water interface, similar to other ancient lakes such as Lake Baikal (Granina et al., 2004).

The OM in the sediments of the DEEP site sequence is predominately of aquatic origin with minor contributions of allochthonous OM supply, as indicated by TOC/TN ratios below 16 (cf. Meyers and Ishiwatari, 1995; Wagner et al., 2009). Thus, high TOC contents in the sediments imply a strong primary productivity in Lake Ohrid, which is also displayed by high amounts of diatom frustules (Wagner et al., 2009) and, accordingly, in high biogenic silica (bSi) contents (Vogel et al., 2010a). A high productivity in the lake requires high temperatures and sufficient nutrient supply to the epilimnion. The nutrient supply to Lake Ohrid is mainly triggered by river inflow (e.g. Matzinger et al., 2006a, b, 2007; Wagner et al., 2009; Vogel et al., 2010a), karstic inflow from Lake Prespa (Matzinger et al., 2006b; Wagner et al., 2009), and by nutrient recycling from the surface sediments (Wagner et al., 2009). Phosphorous recycling from the surface sediments is promoted by anoxic bottom water conditions and mixing can transport phosphorous from the bottom water to the epilimnion (e.g. Wagner et al., 2009). However, mixing also leads to oxidation of OM at the sediment surface and, thus, to lower TOC contents. Hence, low (high) TOC content are be related to an overall lower (higher) productivity and/or to more (less) oxidation of OM and improved (restricted) mixing conditions.

Overall high TOC and bSi contents in lithotype 1 sediments imply a high productivity and high temperatures at Lake Ohrid. Less productivity and/or oxidation of OM can be inferred for sediments of lithotype 2 and 3 from low TOC and bSi contents, and from TOC/TN ratios < 4 (cf. Leng et al., 1999). At Lake Ohrid, low TOC/TN ratios are a result of OM degradation and clay-bound ammonium supply from the catchment, such as observed in core Lz1120 from the southeastern corner of the lake (Holtvoeth et al., 2015).

Good OM preservation, low oxygen availability, and overall poor mixing conditions could have favored sulfide formation, such as pyrite, in lithotype 1 sediments. Pyrite formation can be indicated by a low TOC/TS ratio (cf. Müller, 2001; Wagner et al.,

BGD
12, 15111–15156, 2015

2009). In lithotype 1 sediments, the high TOC/TS ratios correspond to minima in the Fe intensities (cf. Fig. 2), which suggests that iron availability limited the pyrite formation (cf. also Holmer and Storkholm, 2001). This is consistent with temperature dependent magnetic susceptibility measurement on selected samples that indicate minor contents of pyrite throughout the sedimentary sequence (Just et al., 2015). Urban et al. (1999) have shown that early diagenetic sulfur enrichment in OM is low in oligotrophic lakes, as up to 90 % of the produced sulfides can be re-oxidized seasonally or episodically, which affects the sulfur storage over several years. At Lake Ohrid, re-oxidation of sulfides may occur during the mixing season, or under present climate conditions during the irregular complete overturn of the entire water column every few years. If re-oxidation has biased the TOC/TS ratio as an indicator for restricted mixing conditions, the lower ratios in lithotype 2 and 3 sediments are rather a result of the overall low TOC concentrations, which is confirmed by the good correspondence between the TOC/TS ratio and the TOC content.

Elemental intensities of the clastic matter, as obtained from high resolution XRF scanning, can provide information about the sedimentological composition of the deposits, and about erosional processes in the catchment. Variations in the clastic matter content of DEEP site sequence sediments, as inferred from the potassium intensities (K, Fig. 2), can be a result of changing erosion in the catchment, such as it has also been reported from other lakes on the Balkan Peninsula (e.g. Francke et al., 2013). This implies that increased denudation rates could be inferred for lithotype 2 and 3 sediments, while less clastic matter supply occurs in lithotype 1 deposits. However, mutual dilution with authigenic components such as calcite, OM and diatom frustules can bias the potassium record as indicator for denudation and clastic matter supply.

K intensities can occur in K-feldspars and clay minerals. Potassium is mobilized particularly during chemical weathering and pedogenesis, and the residual soils in the catchment become depleted in potassium (Chen et al., 1999). In contrast to K, Zircon mostly occurs in the mineral zirconium, which has a high density and a high resistance against physical and chemical weathering. Thus, the Zr/K ratio provides insights into

BGD
12, 15111–15156, 2015

the intensity of the chemical weathering, which affected the clastic matter in the catchment. Thereby, the Zr/K ratio does not provide information about weathering processes during the time of deposition, as chemically altered minerals may be stored for long time periods in the catchment before they are eroded and transported to a sedimentary basin (cf. also Dosseto et al., 2010). Low Zr/K ratios in lithotype 1 and 2 sediments match with low percentages of the < 4 µm fraction and imply that more coarse detrital matter, predominately consisting of K-rich clastic material from young and moderately chemically weathered soils, were deposited at the DEEP site. In contrast, high Zr/K ratios in lithotype 3 sediments match with high percentages of the < 4 µm fraction and suggest that more fine grained, chemically weathered, and K-depleted clastics from old soils were supplied to the lake.

4.2.2 Event layers

Probable trigger mechanism for MMDs have widely been discussed and encompass earthquakes, delta collapses, flooding events, over steepening of slopes, rock falls, and lake-level fluctuations (e.g. Cohen, 2003; Schnellmann et al., 2006; Girardclos et al., 2007; Sauerbrey et al., 2013). At Lake Ohrid, MMDs in front of the Lini Peninsula (Fig. 1) and in southwestern part of Lake Ohrid were likely triggered by earthquakes (Lindhorst et al., 2012, 2015; Wagner et al., 2012). A strong earthquake might have also triggered the deposition of the MMD in core 1F-4H-3 (cf. Figs. 2 and 3), which is composed of a turbidite succession and an underlying, poorly sorted debrite (after the classification of Mulder and Alexander, 2001). The disturbance generated by a debris flow can cause co-genetic turbidity currents of fine-grained material in front and above the mass movement (Schnellmann et al., 2005; Sauerbrey et al., 2013). As the debrite-turbidite succession occurs at 7.87 m c.d., it likely corresponds to a massive slide complex north of the DEEP site (cf. hydro acoustic profile of Fig. 2 in Wagner et al., 2014). Density flows that enter the Lake Ohrid basin close to the DEEP site from eastern or southern directions have not been observed in hydro-acoustic profiles (cf. Figs. 2 and 3 in Wagner et al., 2014). The three massive MMDs that occur in front of the Lini Peninsula to the west of the DEEP site (cf. Wagner et al., 2012) are likely not related to the debrite-turbidite succession in core 1F-4H-3. The underlying debrite does not occur in overlapping segments of holes 5045-1B, 5045-1C, and 5045-1D. Holes 5045-1B, 5054-1C, and 5045-1D form a N–S transect (40 m distance between each hole), whereas hole 5045-1F is located approximately 70 m to the east. Due to the absence of the debrite deposits in most drill holes and the relatively low thickness in hole 1F, erosional processes at the DEEP site are likely low. In addition, hydroplaning generates a basal water layer below the debris flows, which causes high flow velocities with little basal erosion (Mohrig et al., 1998; Mulder and Alexander, 2001).

The sand lenses and normal graded MMDs (cf. Figs. 2 and 3) can be classified as grain-flow deposits (after the classification of Mulder and Alexander, 2001; Sauerbrey et al., 2013) and are composed of reworked lacustrine sediments from shallow water depths or subaquatic slopes close to riverine inflows. Grain flows that enter the deep parts of the Lake Ohrid basin via the steep slopes might transform into a mesopycnal flow at the boundary of the hypolimmion (cf. also Mulder and Alexander, 2001; Juschus et al., 2009), which prevents erosion of the underlying sediments.

5 Core chronology

The chronostratigraphy for the sediments of the DEEP site sequence down to 247.8 m c.d. was established by using radiometric ages from nine tephra layers (cf. Table 2), and by cross-correlation to orbital parameters (Laskar et al., 2004) and to the global benthic isotope stack LR04 (Lisiecki and Raymo, 2005; Figs. 5 and 6). Correlation of the tephra layers to well-known eruptions from Italian volcanoes by geochemical fingerprint analyses and a re-calibration of $^{40}Ar/^{39}Ar$ ages from the literature provided a robust basis for the age model (Leicher et al., 2015). Thus, the nine tephra layers were used as 1st order tie points.

The chronological information from the nine tephra layers was also used to define cross correlation points to orbital parameters, which were included into the age depth as 2nd order tie points. The tephra layers Y-5, X-6, P11, and A11/12 were deposited when minima in the TOC content and in the TOC/TN ratio can be observed (cf. Fig. 5), and when there is a inflection point (black vertical line in insolation and winter season length plots, Fig. 5) of increasing local summer insolation (21 June, 41° N) and winter season length (21 September to 21 March, Fig. 5). Summer insolation and winter season length have a direct impact on the OM content and the TOC/TN ratio, as they may trigger primary productivity and decomposition. Low insolation and colder temperatures during summer reduce the primary productivity in the lake, but simultaneously, a shorter winter season would have reduced mixing in the lake, which reduces the decomposition of OM and increases TOC and the TOC/TN ratios (cf. Fig. 5, insolation and winter season length minima). A longer winter season improves the mixing, but a strong insolation during summer promotes the primary productivity in the lake, which also results in higher TOC and TOC/TN (cf. Fig. 5, insolation and winter season length maxima). Thus, low OM preservation and low TOC and TOC/TN in the sediments may occur when summer insolation strength and winter season length are balanced, i.e. when both summer insolation and winter season length are at their inflection points. Hence, minima in the TOC content and the TOC/TN ratio were tuned to increasing insolation and winter season lengths.

3rd order tie points were obtained by tuning the LR04 δ^{18}O record to the TIC content, as maxima in the TIC record have a good correspondence with minima in the LR04 δ^{18}O record (cf. Fig. 5), when the stratigraphic positions of the 1st and 2nd order tie points are considered. This is supported by the P11 tephra layer, which has an age of 129 ka. Its position below a TIC peak at ca. 48 m c.d. (cf. Fig. 5) implies that this TIC peak likely corresponds to peak interglacial conditions at 123 ka (MIS 5.5), which is confirmed by results of former sediment core studies (Belmecheri et al., 2009; Vogel et al., 2010a).

Potential explanations for a strong correlation between global benthic δ^{18}O variability and the TIC content in the DEEP site sediments could be a synchronous timing of marine and terrestrial events, or a teleconnection between ice sheet variability and

BGD
12, 15111–15156, 2015

the environmental settings in the Mediterranean Region. Minimum ice sheet expansion (minima in LR04 δ^{18}O) in the Northern Hemisphere and a northern location of the atmospheric circulation patterns and of the Inter-Tropical Convergence Zone (ITCZ), such as it occurs today, could have resulted in maximum summer temperatures at Lake Ohrid. Warm temperatures promote calcite precipitation in the epilimnion. During glacial periods, the northern ice sheet expansion caused a southward shift of the atmospheric circulation patterns (LR04 δ^{18}O maxima), which could have triggered lower temperatures at Lake Ohrid, and less calcite precipitation in the epilimnion.

The nine tephra layers and 45 cross correlation points of 2nd and 3rd order (Supplement) were used for the establishment of an age-depth model. An uncertainty of ±1000 years was applied for each tie point of 2nd and 3rd order in order to account for inaccuracies in the tuning process. For the age depth modeling using the Bacon 2.2 software package (Blaauw and Christen, 2011), overall stable sedimentation rates at the DEEP site (mem.strength = 4, mem.shape = 0.7, thick = 40 cm) and expected sedimentation rates (acc.shape = 1.5, acc.mean = 20) from first age estimations for the DEEP site sequence by Wagner et al. (2014) were considered (cf. Fig. 6). Finally, the age model was evaluated and refined by a detailed comparison with the age- depth model for the downhole logging depth scale (Baumgarten et al., 2015, cf. Fig. 7) by tuning Potassium counts (K) obtained from high-resolution XRF scanning to the spectral gamma radiation (SGR) of potassium (cf. Supplement) in hole 5045-1D (for more details see Baumgarten et al., 2015). The obtained age model reveals that the upper 247.8 m c.d. of the DEEP site sequence comprise the last ca. 640 ka (MIS16).

6 Overview about the paleoenvironmental history of Lake Ohrid

Variations in the TIC, bSi, TOC, K, and Zr/K records of the DEEP site sequence correspond to global and regional climatic variability on glacial–interglacial time scales, such as indicated by a comparison to the global benthic isotope stack LR04 (Lisiecki and Raymo, 2005), to North Greenland isotope record (NGRIP-members, 2004; Barker et al., 2011), and to variations in the arboreal pollen percentage of the Tenaghi Philippon record from Northern Greece (Tzedakis et al., 2006, cf. Fig. 7). In addition to the climatic variability on orbital time scales, a comparison of the individual interglacial and glacial stages allows a first discrimination of the intensity of these stages at Lake Ohrid.

6.1 Interglacials

Between 640 ka and present day, the interglacial sediments of the DEEP site sequence mainly consist of lithotype 1 and 2 sediments. Moderate to high TIC, TOC, and bSi contents in lithotype 1 and 2 sediments imply a moderate to strong primary productivity, and thus, moderate to high temperatures during spring and summer. The overall high temperatures during spring and summer and a longer summer season during interglacial periods likely resulted in an incomplete and restricted mixing of the water column during winter, such as it also persists today. Poor mixing hampers the decomposition of OM and thus, promotes the preservation of TOC and restricts the bacterial CO_2 release at the sediment surface. A reduction in the H_2CO_3 formation and a higher pH in the bottom waters improve the calcite preservation. In addition, interglacial conditions likely promoted high Ca^{2+} and HCO_3^- concentrations and a high pH also in the epilimnion, as warm temperatures increased chemical weathering of the limestones in the catchment and evaporation of lake water. The good correspondence between high TIC during interglacials, which also exhibit overall high δ^{18}O-lake water ($\delta^{18}O_{lw}$) values and indicate a low P/E ratio (Lacey et al., 2015), suggest that evaporation may contribute to high Ca^{2+} and HCO_3^- concentrations in the lake water. Increased evaporation could have also increased the concentration of Si ions in the epilimnion, which could have promoted diatom productivity, as it is indicated by a correspondence between high $\delta^{18}O_{lw}$ and high bSi concentrations. Similar fertilization processes can be observed after the deposition of tephras, when leaching of these tephras results in higher Si concentrations in the lake water (D'Addabbo et al., 2015), and trigger diatom growth in the epilimnion (cf. Jovanovska et al., 2015).

BGD
12, 15111–15156, 2015

Despite intensive chemical weathering and pedogenesis in the catchment during interglacials, low K intensities in lithotype 1 and 2 sediments, along with the stable sedimentation rates despite high accumulation of calcite, bSi, and OM, indicates that the clastic matter supply to the lake basin was low. This is likely a result of low erosion rates in the catchment. Relatively high pollen concentrations in the interglacial sediments of the DEEP site core imply a dense vegetation cover (cf. Fig. 7 and Sadori et al., 2015), which restricted erosion in the catchment of Lake Ohrid. In addition, the low Zr/K ratios and the low proportion of the $< 4\,\mu m$ grain size fraction in lithotype 1 and 2 sediments imply that in particular K-rich minerals and the products of young soils were transported to the lake. This hypothesis is supported by high *S* ratios in interglacial deposits, which indicate a high proportion of primary magnetic minerals (i.e. (titano-)magnetite) from the bedrock in the sediments, whereas the amount of secondary minerals (hematite + goethite) as products of chemical weathering is low (cf. Fig. 7 and Just et al., 2015).

Lithotype 3 deposits with negligible TIC contents only occur at the onsets and terminations of interglacial periods, and during MIS7 and 3 (cf. Fig. 7). The low TIC, TOC, and bSi contents of these sediments correspond to colder periods with a restricted primary productivity. In addition, low temperatures during winter would have improved the mixing, which could promote decomposition of OM in the surface sediments and led to lower TOC and TIC.

Variations of interglacial conditions since 640 ka

Differing OM, bSi, and TIC contents in the interglacial sediments of the DEEP site sequence imply different intensities of interglacials at Lake Ohrid. MIS15 and 13, with high TIC and bSi, and low OM are characterized by strong primary productivity and high temperatures during spring and summer, and decomposition of OM during the mixing season although MIS15 and 13 are regarded as relatively weak interglacials based on the modeled Greenland isotope record (Barker et al., 2011) and the global benthic isotope stack LR04 (Lisiecki and Raymo, 2005, cf. also Fig. 7). On possible explanation could be that the inferred high intensity of these interglacials at Lake Ohrid

BGD
12, 15111–15156, 2015

is due to restricted inflow and precipitation, and high evaporation, as it is suggested by high $\delta^{18}O_{lw}$ concentrations (Lacey et al., 2015). In addition, the high TIC and bSi concentrations could also be a result of the lower TOC contents and of mutual dilution with OM.

During the first part of MIS11, between 420 and 400 ka, highest TIC concentrations along with moderate and high bSi and TOC concentration imply highest productivity (high TOC) and highest temperatures (highest TIC), while biogenic silica preservation in the sediments is restricted. This is consistent with other records, where strongest interglacial conditions and highest temperatures since 640 ka are reported for the onset of MIS11 (Lang and Wolff, 2011).

TIC concentration during the second phase of MIS 11, between 400 and 374 ka, and during MIS9 and 7 are generally lower and mostly restricted to distinct peaks. This implies overall less calcite precipitation, less primary productivity, and lower temperatures at Lake Ohrid. This is consistent with the low bSi concentrations, but not with the high TOC contents, and with relatively stronger interglacials subsequent to the MBE inferred from the modeled North Greenland isotope record (Barker et al., 2011) and the LR04 stack (Lisiecki and Raymo, 2005). The temperatures during the second phase of MIS11 and during MIS9 and 7 were likely lower compared to the first phase of MIS11 as indicated by the TIC record (cf. Fig. 7), and in addition the somewhat lower TIC and bSi contents also correspond to lower $\delta^{18}O_{lw}$ concentrations in the Lake Ohrid sediments, which imply that this interglacial periods are isotopically fresher and less evaporated than the previous interglacial periods (Lacey et al., 2015).

Overall high TIC, TOC, and bSi concentrations during MIS5 imply a strong primary productivity in the eplimnion and high temperatures during spring and summer. $\delta^{18}O_{lw}$ during MIS5 is notably higher compared to the two previous interglacial periods (Lacey et al., 2015) and indicates a low P/E ratio. In particular the onset of MIS5 is reported to be the strongest interglacial period during the last 640 ka in marine records (Lang and Wolff, 2011), which is also indicated in the North Greenland temperature variations (NGRIP-members, 2004; Barker et al., 2011), and in the global benthic isotope

BGD
12, 15111–15156, 2015

stack LR04 (Lisiecki and Raymo, 2005), and correspond to high TIC, TOC, and bSi concentrations in the DEEP site sequence.

6.2 Glacials

Glacial periods between 640 ka and today are characterized by predominant deposition of lithotype 3 sediments, with rare occurrence of lithotype 1 and 2 sediments in MIS14 and 8, when TIC contents are higher. Low TOC and bSi and negligible TIC contents in lithotype 3 sediments imply low primary productivity and low temperatures during glacial periods. Some minor fluctuations in productivity and temperature are indicated by TOC and bSi. They are not documented in TIC, as oxidation of OM at the sediment surface due to intensified and prolonged mixing, which is indicated by TOC/TN ratios < 4, may have led to a slight decrease of the bottom water pH and dissolution of calcite precipitated from the epilimnion. Dissolution of calcite and the existence of a threshold can also explain the delayed increase of TIC compared to TOC and bSi at the transitions of MIS16, 12, 10, 8, 6, and 2 into the following interglacials.

High K, a high proportion of the fine fraction $< 4\,\mu m$, and stable sedimentation rates despite low calcite, OM and bSi content in the glacial sediments, indicate high input of clastic terrigenous matter and increased erosion in the catchment. Furthermore, the high Zr/K ratios suggest the supply of K-depleted, intensively weathered soils from the catchment, which is supported by a higher hematite + goethite to magnetite ratio (low *S* ratio) in glacial deposits of the DEEP site sequence (cf. Fig. 7 and Just et al., 2015). The enhanced erosion of intensively weathered clastic material can be explained by less dense vegetation cover in the catchment, such as implied by low pollen concentrations in the DEEP site sequence in most of the glacial periods (cf. Fig. 7), and by the existence of local ice caps in the surrounding mountains of Lake Ohrid, as indicated by moraines in the catchment, which are though to have formed during the last glacial cycle (Ribolini et al., 2011).

BGD
12, 15111–15156, 2015

Variations of glacial conditions since 640 ka

As TIC is affected by dissolution and indicate negligible calcite concentrations, information about the severity of the individual glacials at Lake Ohrid can only be inferred from TOC and bSi. Minima in the TOC and bSi imply that most severe glacial conditions at Lake Ohrid occurred at the end of MIS16, and during MIS12, 10, and 6. Somewhat higher bSi and TOC in parts of MIS14 and 8, and in MIS6, 4, and 2 imply less severe glacial conditions. This implies that the finding of glacial moraines from MIS2 (Ribolini et al., 2011) is probably only due to better preservation of these glacial features compared to the older glacials. Interglacial-like conditions with higher primary productivity and reduced oxidation of OM in the surface sediments prevailed at the occurrence of lithotype 1 and 2 sedimentation, i.e. between 563 and 540 ka during MIS14, and between 292 and 282 ka during MIS 8.

The frequent occurrence of MMDs between 280 and 241 ka and between 160 and 130 ka implies significant lake level fluctuations during MIS8 and 6. During the first period (MIS8), distinct fluctuations in the AP pollen percentages of the Tenaghi Philippon pollen record (Tzedakis et al., 2006) correspond to similar fluctuations in the pollen concentrations in the DEEP site sequence (cf. Fig. 7, and Sadori et al., 2015) and probably indicate a shift from cold and dry to more warm and humid conditions in northern Greece and at Lake Ohrid. During MIS6, a 60 m lower lake-level compared to present conditions, and a subsequent lake level rise during late MIS6 or during the transition from MIS6 to MIS5 is reported from hydro-acoustic and sediment core analyses from the northeastern corner of Lake Ohrid (Lindhorst et al., 2010). This is in agreement with pollen data (Sadori et al., 2015), which suggest that quite arid conditions took place during MIS6.

The general observation that MIS16 and 12 were the most severe glacials is in broad agreement with other records, such as the North Greenland isotope record (Barker et al., 2011), the global benthic stack LR04 (Lisiecki and Raymo, 2005), and the Tenaghi Philippon pollen record (Tzedakis et al., 2006). Furthermore, TOC, bSi and greigite in the Lake Ohrid DEEP site sequence support that MIS10 was more severe than MIS6, as syn-sedimentary formation of greigite during the older glacial period is likely linked to a combination of low productivity and improved mixing conditions in the lake (Just et al., 2015). However, the idea that MIS10 is more severe than MIS6 differs from the pollen records from the same core (Sadori et al., 2015) and from Tenaghi Philippon (Tzedakis et al., 2006), as both archives suggest more harsh conditions during MIS6. The pollen record from the DEEP site sequence also imply a strong aridity during MIS6 (Sadori et al., 2015), which is consistent with a low lake level of Lake Ohrid as implied by the frequent occurrence of MMDs between 160 and 130 ka, and the results of the sediment core and hydro-acoustic study in the northeastern corner of the lake (Lindhorst et al., 2010). This implies that the dry conditions during MIS6 are probably not mirrored in TOC, bSi, and greigite concentration.

7 Summary and conclusion

The investigated sediment succession between 247.8 m c.d. and the sediment surface from the DEEP site in the central part of Lake Ohrid provides a valuable archive of environmental and climatological change for the last 640 ka. An age model was established using chronological tie points from nine tephra layers, and by tuning biogeochemical proxy data to orbital parameters and to the global benthic isotope stack LR04. The imprint of environmental change on the lithological, sedimentological, and (bio-)geochemistry data can be used to unravel the lake's history including the development of the Lake Ohrid basin, and the climatological variability on the Balkan Peninsula.

The lithological, sedimentological, and geochemical data from the DEEP site sequence imply that Lake Ohrid did not experience major catastrophic events such as extreme lake-level low stands or desiccation events during the last 640 ka. Hiatuses are absent and the DEEP site sequence provides an undisturbed archive of environmental and climatological change.

Based on the initial core description and the calcite content, the hemipelagic sediments from the DEEP site sequence can be classified into the three lithotypes. This classification is supported by variations in the (bio-)geochemistry data and follows climate variations on glacial/interglacial time scales. Overall, interglacial periods are characterized by high primary productivity during summer, restricted mixing during winter, and low erosion in the catchment. During glacial periods, the primary productivity is low, intense mixing of the water column promotes the decomposition of OM, which may have lowered the water pH and led to dissolution of calcite at the sediment surface. Enhanced erosion of interglacial soils and higher clastic matter input into the lake during glacial periods can be explained by a less dense vegetation cover in the catchment and melt water run-off due to the existence of local ice caps on the surrounding mountains.

Following a strong primary productivity during spring and summer, highest interglacial temperatures can be inferred for the first part of MIS11, and for MIS5. In contrast, somewhat lower spring and summer temperatures are observed for MIS15, 13, 9, and 7. The data also suggested that high ion and nutrient concentrations in the lake water promote calcite precipitation and diatom growth in the epilmnion during MIS15, 13, and 5, whereas less evaporated interglacial periods exhibit lower TIC and bSi contents (MIS9 and 7).

Most severe glacial conditions at Lake Ohrid persisted during MIS16, 12, 10, and 6, whereas somewhat warmer temperatures can be inferred for MIS14, 8, 4, and 3. A low lake level implies dry conditions during MIS6. Interglacial-like conditions occurred during parts of MIS14 and 8, respectively.

The Supplement related to this article is available online at doi:10.5194/bgd-12-15111-2015-supplement.

Acknowledgements. The SCOPSCO Lake Ohrid drilling campaign was funded by ICDP, the German Ministry of Higher Education and Research, the German Research Foundation, the

University of Cologne, the British Geological Survey, the INGV and CNR (both Italy), and the governments of the republics of Macedonia (FYROM) and Albania. Logistic support was provided by the Hydrobiological Institute in Ohrid. Drilling was carried out by Drilling, Observation and Sampling of the Earth's Continental Crust's (DOSECC) and using the Deep Lake Drilling System (DLDS). Special thanks are due to Beau Marshall and the drilling team. Ali Skinner and Martin Melles provided immense help and advice during logistic preparation and the drilling operation. Furthermore, the authors thank Ronald Conze (GFZ Potsdam), Dorothea Klinghardt (University of Cologne), Nicole Mantke (University of Cologne), Volker Wennrich (University of Cologne), and various student assistants for their immense support during the core processing and the analytical work at the University of Cologne. The playnological specialists of the Lake Ohrid community contributed with immense work to the pollen analyses on the DEEP site sequence, the reader is referred to Sadori et al. (2015) for a detailed list of all involved scientists. Acknowledged are also Andreas Koutsodendris (University of Heidelberg) and Alessia Masi (University of Rome) for the pollen plot in Fig. 7 and for helpful discussions.

References

Albrecht, C. and Wilke, T.: Ancient Lake Ohrid: biodiversity and evolution, Dev. Hydrob., 205, 103–140, doi:10.1007/978-1-4020-9582-5_9, 2009.

Aliaj, S., Baldassarre, G., and Shkupi, D.: Quaternary subsidence zones in Albania: some case studies, B. Eng. Geol. Environ., 59, 313–318, doi:10.1007/s100640000063, 2001.

Arnaud, F., Revel, M., Chapron, E., Desmet, M., and Tribovillard, N.: 7200 years of Rhone river flooding activity in Lake Le Bourget, France: a high-resolution sediment record of NW Alps hydrology, Holocene, 15, 420–428, doi:10.1191/0959683605hl801rp, 2005.

Barker, S., Knorr, G., Edwards, R. L., Parrenin, F., Putnam, A. E., Skinner, L. C., Wolff, E., and Ziegler, M.: 800,000 years of abrupt climate variability, Science, 334, 347–351, doi:10.1126/science.1203580, 2011.

Baumgarten, H., Wonik, T., Tanner, D. C., Francke, A., Wagner, B., Zanchetta, G., Sulpizio, R., Giaccio, B., and Nomade, S.: Age depth-model for the past 630 ka in Lake Ohrid (Macedonia/Albania) based on cyclostratigraphic analysis of downhole gamma ray data, Biogeosciences Discuss., 12, 7671–7703, doi:10.5194/bgd-12-7671-2015, 2015.

Belmecheri, S., Namiotko, T., Robert, C., von Grafenstein, U., and Danielopol, D. L.: Climate controlled ostracod preservation in Lake Ohrid (Albania, Macedonia), Palaeogeogr. Palaeocl., 277, 236–245, doi:10.1016/j.palaeo.2009.04.013, 2009.
Blaauw, M. and Christen, J. A.: Flexible paleoclimate age-depth models using an autoregressive gamma process, Bayesian Analysis, 6, 457–474, doi:10.1214/ba/1339616472, 2011.
Blott, S. J. and Pye, K.: GRADISTAT: a grain size distribution and statistics package for the analysis of unconsolidated sediments, Earth Surf. Proc. Land., 26, 1237–1248, doi:10.1002/esp.261, 2001.
Chen, J., An, Z., and Head, J.: Variation of Rb/Sr ratios in the loess-paleosol sequences of central China during the last 130,000 years and their implications for monsoon paleoclimatology, Quaternary Res., 51, 215–219, doi:10.1006/qres.1999.2038, 1999.
Cohen, H.: Paleolimnology: The History and Evolution of Lake Systems, Oxford University Press, New York, 2003.
D'Addabbo, M., Sulpizio, R., Guidi, M., Capitani, G., Mantecca, P., and Zanchetta, G.: Ash leachates from some recent eruptions of Mount Etna (Italy) and Popocatépetl (Mexico) volcanoes and their impact on amphibian living freshwater organisms, Biogeosciences Discuss., 12, 13241–13282, doi:10.5194/bgd-12-13241-2015, 2015.
Dosseto, A., Hesse, P. P., Maher, K., Fryirs, K., and Turner, S.: Climatic and vegetation control on sediment dynamics during the last glacial cycle, Geology, 38, 395–398, doi:10.1130/g30708.1, 2010.
EPICA-members: Eight glacial cycles from an Antarctic ice core, Nature, 429, 623–628, doi:10.1038/nature02599, 2004.
Francke, A., Wagner, B., Leng, M. J., and Rethemeyer, J.: A Late Glacial to Holocene record of environmental change from Lake Dojran (Macedonia, Greece), Clim. Past, 9, 481–498, doi:10.5194/cp-9-481-2013, 2013.
Girardclos, S., Schmidt, O. T., Sturm, M., Ariztegui, D., Pugin, A., and Anselmetti, F. S.: The 1996 AD delta collapse and large turbidite in Lake Brienz, Mar. Geol., 241, 137–154, doi:10.1016/j.margeo.2007.03.011, 2007.
Granina, L., Müller, B., and Wehrli, B.: Origin and dynamics of Fe and Mn sedimentary layers in Lake Baikal, Chem. Geol., 205, 55–72, doi:10.1016/j.chemgeo.2003.12.018, 2004.
Hoffmann, N., Reicherter, K., Fernández-Steeger, T., and Grützner, C.: Evolution of ancient Lake Ohrid: a tectonic perspective, Biogeosciences, 7, 3377–3386, doi:10.5194/bg-7-3377-2010, 2010.

BGD
12, 15111–15156, 2015

Title Page
Abstract | Introduction
Conclusions | References
Tables | Figures
◀| |▶
◀ ▶
Back | Close
Full Screen / Esc
Printer-friendly Version
Interactive Discussion

Holmer, M. and Storkholm, P.: Sulphate reduction and sulphur cycling in lake sediments: a review, Freshwater Biol., 46, 431–451, doi:10.1046/j.1365-2427.2001.00687.x, 2001.
Holtvoeth, J., Rushworth, D., Imeri, A., Cara, M., Vogel, H., Wagner, T., and Wolff, G. A.: Improved end-member characterization of modern organic matter pools in the Ohrid Basin (Albania, Macedonia) and evaluation of new palaeoenvironmental proxies, Biogeosciences Discuss., 12, 12975–13039, doi:10.5194/bgd-12-12975-2015, 2015.
Jovanovska, E., Cvetkoska, A., Levkov, Z., Sulpizio, R., Hauffe, T., Wagner, B., Albrecht, C., and Wilke, T.: Testing diatom response to tephra influx in Lake Ohrid (Macedonia, Albania), Biogeosciences Discuss., in preparation, 2015.
Juschus, O., Melles, M., Gebhardt, A. C., and Niessen, F.: Late Quaternary mass movement events in Lake El'gygytgyn, north-eastern Siberia, Sedimentology, 56, 2155–2174, doi:10.1111/j.1365-3091.2009.01074.x, 2009.
Just, J., Nowaczyk, N., Francke, A., Sagnotti, L., and Wagner, B.: Climatic control on the occurrence of high-coercivity magnetic minerals and preservation of greigite in a 640 ka sediment sequence from Lake Ohrid (Balkans), Biogeosciences Discuss., 12, 14215–14243, doi:10.5194/bgd-12-14215-2015, 2015.
Lacey, J. H., Leng, M. J., Francke, A., Sloane, H. J., Milodowski, A., Vogel, H., Baumgarten, H., and Wagner, B.: Mediterranean climate since the Middle Pleistocene: a 640 ka stable isotope record from Lake Ohrid (Albania/Macedonia), Biogeosciences Discuss., 12, 13427–13481, doi:10.5194/bgd-12-13427-2015, 2015.
Lang, N. and Wolff, E. W.: Interglacial and glacial variability from the last 800 ka in marine, ice and terrestrial archives, Clim. Past, 7, 361–380, doi:10.5194/cp-7-361-2011, 2011.
Laskar, J., Robutel, P., Joutel, F., Gastineau, M., Correia, A. C. M., and Levrard, B.: A long-term numerical solution for the insolation quantities of the Earth, Astron. Astrophys., 428, 261–285, doi:10.1051/0004-6361:20041335, 2004.
Leicher, N., Zanchetta, G., Sulpizio, R., Giaccio, B., Wagner, B., Nomade, S., and Francke, A.: First tephrostratigraphic results of the DEEP site record in Lake Ohrid, Macedonia, Biogeosciences, in press, 2015.
Leng, M. J., Roberts, N., Reed, J. M., and Sloane, H. J.: Late Quaternary palaeohydrology of the Konya Basin, Turkey, based on isotope studies of modern hydrology and lacustrine carbonates, J. Paleolimnol., 22, 187–204, doi:10.1023/a:1008024127346, 1999.
Leng, M. J., Baneschi, I., Zanchetta, G., Jex, C. N., Wagner, B., and Vogel, H.: Late Quaternary palaeoenvironmental reconstruction from Lakes Ohrid and Prespa (Macedonia/Albania

border) using stable isotopes, Biogeosciences, 7, 3109–3122, doi:10.5194/bg-7-3109-2010, 2010.
Leng, M. J., Wagner, B., Boehm, A., Panagiotopoulos, K., Vane, C. H., Snelling, A., Haidon, C., Woodley, E., Vogel, H., Zanchetta, G., and Baneschi, I.: Understanding past climatic and hydrological variability in the Mediterranean from Lake Prespa sediment isotope and geochemical record over the Last Glacial cycle, Quaternary Sci. Rev., 66, 123–136, doi:10.1016/j.quascirev.2012.07.015, 2013.
Lindhorst, K., Vogel, H., Krastel, S., Wagner, B., Hilgers, A., Zander, A., Schwenk, T., Wessels, M., and Daut, G.: Stratigraphic analysis of lake level fluctuations in Lake Ohrid: an integration of high resolution hydro-acoustic data and sediment cores, Biogeosciences, 7, 3531–3548, doi:10.5194/bg-7-3531-2010, 2010.
Lindhorst, K., Gruen, M., Krastel, S., and Schwenk, T.: Hydroacoustic analysis of mass wasting deposits in Lake Ohrid (FYR Macedonia/Albania), in: Submarine Mass Movements and Their Consequences, edited by: Yamada, Y., Kawamura, K., Ikehara, K., Ogawa, Y., Urgeles, R., Mosher, D., Chaytor, J., Strasser, and M., Springer, the Netherlands, 245–253, 2012.
Lindhorst, K., Krastel, S., Reicherter, K., Stipp, M., Wagner, B., and Schwenk, T.: Sedimentary and tectonic evolution of Lake Ohrid (Macedonia/Albania), Basin Res., 27, 84–101, doi:10.1111/bre.12063, 2015.
Lisiecki, L. E. and Raymo, M. E.: A Pliocene–Pleistocene stack of 57 globally distributed benthic δ^{18}O records, Paleoceanography, 20, PA1003, doi:10.1029/2004pa001071, 2005.
Matzinger, A., Spirkovski, Z., Patceva, S., and Wüest, A.: Sensitivity of ancient Lake Ohrid to local anthropogenic impacts and global warming, J. Great Lakes Res., 32, 158–179, doi:10.3394/0380-1330(2006)32[158:SOALOT]2.0.CO;2, 2006a.
Matzinger, A., Jordanoski, M., Veljanoska-Sarafiloska, E., Sturm, M., Müller, B., and Wüest, A.: Is Lake Prespa jeopardizing the ecosystem of ancient Lake Ohrid?, Hydrobiologia, 553, 89–109, doi:10.1007/s10750-005-6427-9, 2006b.
Matzinger, A., Schmid, M., Veljanoska-Sarafiloska, E., Patceva, S., Guseska, D., Wagner, B., Müller, B., Sturm, M., and Wüest, A.: Eutrophication of ancient Lake Ohrid: global warming amplifies detrimental effects of increased nutrient inputs, Limnol. Oceanogr., 52, 338–353, 2007.
Melles, M., Brigham-Grette, J., Minyuk, P., Nowaczyk, N., Wennrich, V., Deconto, R., Andersen, P., Andreev, A. A., Coletti, A., Cook, T., Haltia-Hovi, E., Kukkonen, M., Lozhkin, A., Rosén, P., Tarasov, P., Vogel, H., and Wagner, B.: 2.8 million years of Artic climate change

BGD
12, 15111–15156, 2015

Sedimentological processes and environmental variability at Lake Ohrid

A. Francke et al.

from Lake El'gygytgyn, NE Russia, Science, 337, 315–320, doi:10.1126/science.1222135, 2012.
Meyer-Jacob, C., Vogel, H., Boxberg, F., Rosén, P., Weber, M., and Bindler, R.: Independent measurement of biogenic silica in sediments by FTIR spectroscopy and PLS regression, J. Paleolimnol., 52, 245–255, doi:10.1007/s10933-014-9791-5, 2014.
Meyers, P. A. and Ishiwatari, R.: Organic matter accumulation records in lake sediments, in: Physics and Chemistry of Lakes, edited by: Lerman, A., Imboden, D. M., and Gat, J. R., Springer Verlag, Berlin, Heidelberg, New York, 279–328., 1995.
Mohrig, D., Ellis, C., Parker, G., Whipple, K. X., and Hondzo, M.: Hydroplaning of subaqueous debris flows, Geol. Soc. Am. Bull., 110, 387–394, doi:10.1130/0016-7606(1998)110<0387:HOSDF>2.3.CO;2, 1998.
Mulder, T. and Alexander, J.: The physical character of subaqueous sedimentary density flows and their deposits, Sedimentology, 48, 269–299, doi:10.1046/j.1365-3091.2001.00360.x, 2001.
Müller, A.: Late- and postglacial sea-level change and paleoenvironments in the Oder Estuary, southern Baltic Sea, Quaternary Res., 55, 86–96, doi:10.1006/qres.2000.2189, 2001.
Müller, B., Wang, Y., and Wehrli, B.: Cycling of calcite in hard water lakes of different trophic states, Limnol. Oceanogr., 51, 1678–1688, doi:10.4319/lo.2006.51.4.1678, 2006.
NGRIP-members: High-resolution record of Northern Hemisphere climate extending into the last interglacial period, Nature, 431, 147–151, doi:10.1038/nature02805, 2004.
Panagiotopoulos, K., Aufgebauer, A., Schäbitz, F., and Wagner, B.: Vegetation and climate history of the Lake Prespa region since the Lateglacial, Quatern. Int., 292, 157–169, doi:10.1016/j.quaint.2012.05.048, 2013.
Prokopenko, A. A., Hinnov, L. A., Williams, D. F., and Kuzmin, M. I.: Orbital forcing of continental climate during the Pleistocene: a complete astronomically tuned climatic record from Lake Baikal, SE Siberia, Quaternary Sci. Rev., 25, 3431–3457, doi:10.1016/j.quascirev.2006.10.002, 2006.
Raymo, M. E., Lisiecki, L. E., and Nisancioglu, K. H.: Plio–Pleistocene ice volume, Antarctic climate, and the global δ^{18}O record, Science, 313, 492–495, doi:10.1126/science.1123296, 2006.
Reicherter, K., Hoffmann, N., Lindhorst, K., Krastel, S., Fernandez-Steeger, T., Grützner, C., and Wiatr, T.: Active basins and neotectonics: morphotectonics of the Lake Ohrid

BGD
12, 15111–15156, 2015

Sedimentological processes and environmental variability at Lake Ohrid

A. Francke et al.

Basin (FYROM and Albania), Z. Dtsch. Ges. Geowiss., 162, 217–234, doi:10.1127/1860-1804/2011/0162-0217, 2011.
Ribolini, A., Isola, I., Zanchetta, G., Bini, M., and Sulpizio, R.: Glacial feature on the Galicica Mountains, Macedonia: preliminary report, Geogr. Fis. Din. Quat., 34, 247–255, doi:10.4461/GFDQ.2011.34.22, 2011.
Sadori, L., Koutsodendris, A., Masi, A., Bertini, A., Combourieu Nebout, N., Francke, A., Kouli, K., Joannin, S., Mercuri, A. M., Panagiotopoulos, K., Peyron, O., Torri, P., Wagner, B., Zanchetta, G., and Donders, T. H.: Palaeoenvironmental changes detected by palynology in the last 500 ky at Lake Ohrid (southern Europe), Biogeosciences Discuss., in preparation, 2015.
Sauerbrey, M. A., Juschus, O., Gebhardt, A. C., Wennrich, V., Nowaczyk, N. R., and Melles, M.: Mass movement deposits in the 3.6 Ma sediment record of Lake El'gygytgyn, Far East Russian Arctic, Clim. Past, 9, 1949–1967, doi:10.5194/cp-9-1949-2013, 2013.
Schnellmann, M., Anselmetti, F. S., Giardini, D., and McKenzie, J. A.: Mass movement-induced fold-and-thrust belt structures in unconsolidated sediments in Lake Lucerne (Switzerland), Sedimentology, 52, 271–289, doi:10.1111/j.1365-3091.2004.00694.x, 2005.
Schnellmann, M., Anselmetti, F., Giardini, D., and McKenzie, J.: 15,000 years of mass-movement history in Lake Lucerne: implications for seismic and tsunami hazards, Eclogae Geol. Helv., 99, 409–428, doi:10.1007/s00015-006-1196-7, 2006.
Stein, M., Ben-Avraham, Z., Goldstein, S., Agnon, A., Ariztegui, D., Brauer, A., Haug, G., Ito, E., and Yasuda, Y.: Deep drilling at the Dead Sea, Sci. Dril., 11, 46–47, doi:10.5194/sd-11-46-2011, 2011.
Stockhecke, M., Sturm, M., Brunner, I., Schmincke, H.-U., Sumita, M., Kipfer, R., Cukur, D., Kwiecien, O., and Anselmetti, F. S.: Sedimentary evolution and environmental history of Lake Van (Turkey) over the past 600 000 years, Sedimentology, 61, 1830–1861, doi:10.1111/sed.12118, 2014a.
Stockhecke, M., Kwiecien, O., Vigliotti, L., Anselmetti, F. S., Beer, J., Çağatay, M. N., Channell, J. E. T., Kipfer, R., Lachner, J., Litt, T., Pickarski, N., and Sturm, M.: Chronostratigraphy of the 600,000 year old continental record of Lake Van (Turkey), Quaternary Sci. Rev., 104, 8–17, doi:10.1016/j.quascirev.2014.04.008, 2014b.
Sulpizio, R., Zanchetta, G., D'Orazio, M., Vogel, H., and Wagner, B.: Tephrostratigraphy and tephrochronology of lakes Ohrid and Prespa, Balkans, Biogeosciences, 7, 3273–3288, doi:10.5194/bg-7-3273-2010, 2010.

BGD
12, 15111–15156, 2015

Tzedakis, P. C., Hooghiemstra, H., and Pälike, H.: The last 1.35 million years at Tenaghi Philippon: revised chronostratigraphy and long-term vegetation trends, Quaternary Sci. Rev., 25, 3416–3430, doi:10.1016/j.quascirev.2006.09.002, 2006.
Urban, N. R., Ernst, K., and Bernasconi, S.: Addition of sulfur to organic matter during early diagenesis of lake sediments, Geochim. Cosmochim. Ac., 63, 837–853, doi:10.1016/s0016-7037(98)00306-8, 1999.
Vogel, H., Wagner, B., Zanchetta, G., Sulpizio, R., and Rosén, P.: A paleoclimate record with tephrochronological age control for the last glacial–interglacial cycle from Lake Ohrid, Albania and Macedonia, J. Paleolimnol., 44, 295–310, doi:10.1007/s10933-009-9404-x, 2010a.
Vogel, H., Wessels, M., Albrecht, C., Stich, H.-B., and Wagner, B.: Spatial variability of recent sedimentation in Lake Ohrid (Albania/Macedonia), Biogeosciences, 7, 3333–3342, doi:10.5194/bg-7-3333-2010, 2010b.
Vogel, H., Zanchetta, G., Sulpizio, R., Wagner, B., and Nowaczyk, N.: A tephrostratigraphic record for the last glacial–interglacial cycle from Lake Ohrid, Albania and Macedonia, J. Quaternary Sci., 25, 320–338, doi:10.1002/jqs.1311, 2010c.
Wagner, B., Reicherter, K., Daut, G., Wessels, M., Matzinger, A., Schwalb, A., Spirkovski, Z., and Sanxhaku, M.: The potential of Lake Ohrid for long-term palaeoenvironmental reconstructions, Palaeogeogr. Palaeocl., 259, 341–356, doi:10.1016/j.palaeo.2007.10.015, 2008.
Wagner, B., Lotter, A. F., Nowaczyk, N., Reed, J. M., Schwalb, A., Sulpizio, R., Valsecchi, V., Wessels, M., and Zanchetta, G.: A 40,000-year record of environmental change from ancient Lake Ohrid (Albania and Macedonia), J. Paleolimnol., 41, 407–430, doi:10.1007/s10933-008-9234-2, 2009.
Wagner, B., Francke, A., Sulpizio, R., Zanchetta, G., Lindhorst, K., Krastel, S., Vogel, H., Rethemeyer, J., Daut, G., Grazhdani, A., Lushaj, B., and Trajanovski, S.: Possible earthquake trigger for 6th century mass wasting deposit at Lake Ohrid (Macedonia/Albania), Clim. Past, 8, 2069–2078, doi:10.5194/cp-8-2069-2012, 2012.
Wagner, B., Wilke, T., Krastel, S., Zanchetta, G., Sulpizio, R., Reicherter, K., Leng, M. J., Grazhdani, A., Trajanovski, S., Francke, A., Lindhorst, K., Levkov, Z., Cvetkoska, A., Reed, J. M., Zhang, X., Lacey, J. H., Wonik, T., Baumgarten, H., and Vogel, H.: The SCOPSCO drilling project recovers more than 1.2 million years of history from Lake Ohrid, Sci. Dril., 17, 19–29, doi:10.5194/sd-17-19-2014, 2014.
Watzin, M., Puka, V., and Naumoski, T.: Lake Ohrid and its Watershed, State of the Environment Report, Lake Ohrid Conservation Project, Tirana, Albania and Ohrid, Macedonia, 2002.

BGD
12, 15111–15156, 2015

Title Page
Abstract | Introduction
Conclusions | References
Tables | Figures
◂◂ | ▸▸
◂ | ▸
Back | Close
Full Screen / Esc
Printer-friendly Version
Interactive Discussion

Wennrich, V., Minyuk, P. S., Borkhodoev, V., Francke, A., Ritter, B., Nowaczyk, N. R., Sauerbrey, M. A., Brigham-Grette, J., and Melles, M.: Pliocene to Pleistocene climate and environmental history of Lake El'gygytgyn, Far East Russian Arctic, based on high-resolution inorganic geochemistry data, Clim. Past, 10, 1381–1399, doi:10.5194/cp-10-1381-2014, 2014.
Wold, S., Sjöström, M., and Eriksson, L.: PLS-regression: a basic tool of chemometrics, Chemometr. Intell. Lab., 58, 109–130, doi:10.1016/S0169-7439(01)00155-1, 2001.

BGD
12, 15111–15156, 2015

Table 1. The contributions of the different core sections to the DEEP site profile.

Hole	Number of core runs	Percent of core runs	Number of sections	Percent of sections
Co1261	2	1.1 %	2	0.5 %
5045-1B	26	14.2 %	50	12.9 %
5045-1C	72	39.3 %	137	35.3 %
5045-1D	75	41.0 %	184	47.4 %
5045-1F	8	4.4 %	15	3.9 %
$\sum$	183		388	

BGD
12, 15111–15156, 2015

Table 2. Correlated tephra layer in the DEEP site sequence according to Leicher et al. (2015). $^{40}Ar/^{39}Ar$ ages from the literature were recalculated on a 2σ confidence level (Leicher et al., 2015).

Ohrid Tephra (m c.d.)	Correlated eruption/tephra	Recalculated $^{40}Ar/^{39}Ar$ age (ka)
2.773	Mercato	8.540 ± 0.05 *
11.507	Y-3	29.05 ± 0.37 *
16.933	Y-5	39.6 ± 0.1
43.513	X-6	109 ± 2
49.947	P11	129 ± 6
61.726	Vico B	162 ± 6
181.769	Pozzolane Rosse	457 ± 2
201.049	Sabatini Fall A	496 ± 3
201.782	A11/A12	511 ± 6

* Calibrated ^{14}C age.

BGD
12, 15111–15156, 2015

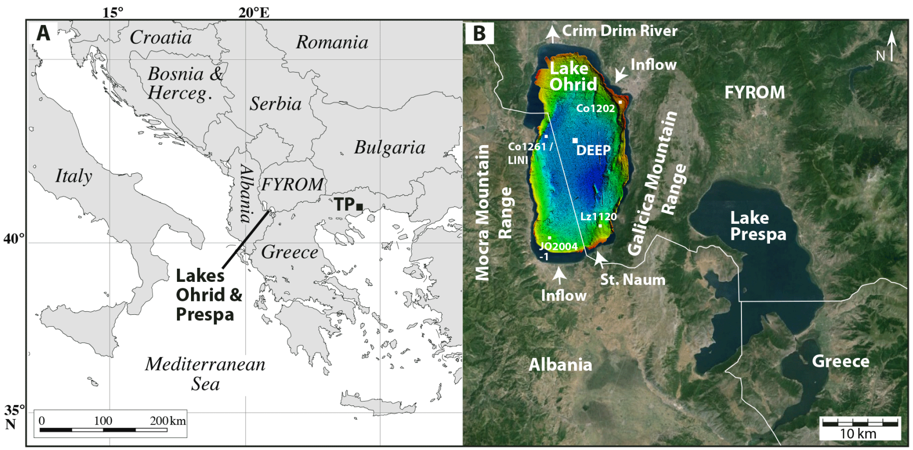

Figure 1. (a) Location of lakes Ohrid and Prespa on the Balkan Peninsula. **(b)** Map of the area of lakes Ohrid and Prespa and bathymetric map of Lake Ohrid. Marked in white are the DEEP site and the short cores Lz1120 (Wagner et al., 2009), Co1202 (Vogel et al., 2010a), and LO2004-1 (Belmecheri et al., 2009). TP: Tenaghi Pilippon pollen record.

BGD
12, 15111–15156, 2015

Sedimentological processes and environmental variability at Lake Ohrid

A. Francke et al.

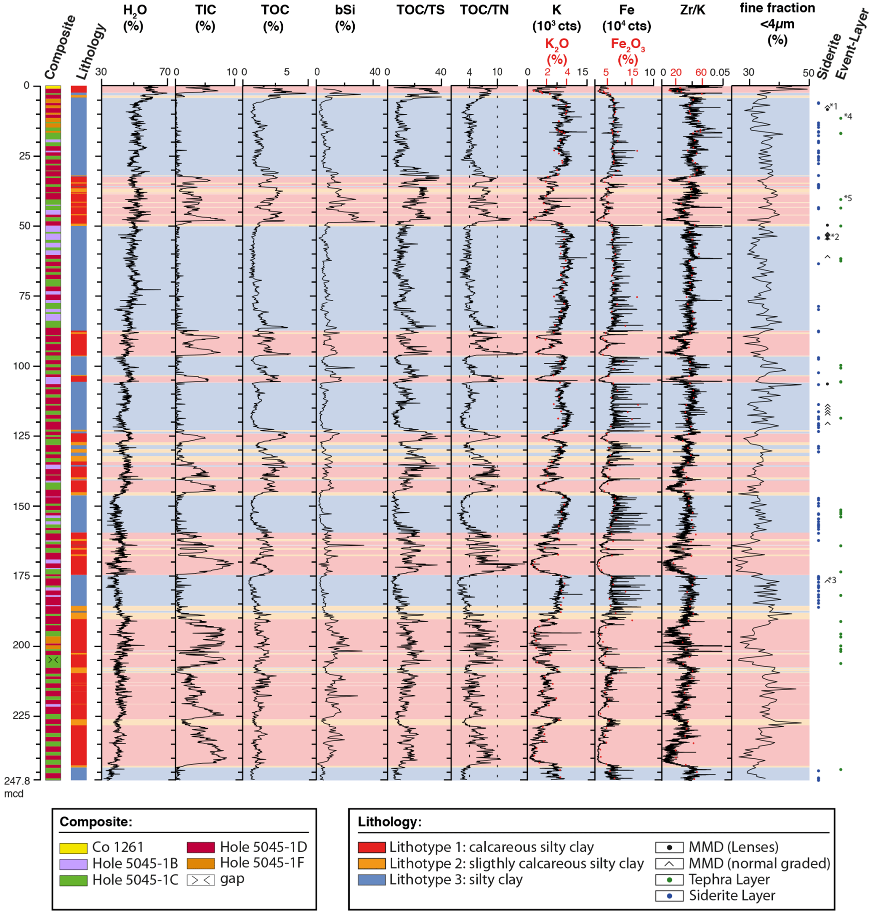

BGD
12, 15111–15156, 2015

Sedimentological processes and environmental variability at Lake Ohrid

A. Francke et al.

Title Page
Abstract
Introduction
Conclusions
References
Tables
Figures
◀I
▶I
◀
▶
Back
Close
Full Screen / Esc
Printer-friendly Version
Interactive Discussion

Figure 2. Variations of the lithological and (bio-)geochemical proxy data of the DEEP site sequence plotted against meter composite depth (m c.d.). The core composite profile of the DEEP site sediment sequence consists of core sections from core Co1261 (upper 0.93 m c.d.), and of core sections from holes 5045-1B, 5045-1C, 5045-1D, and 5045-1F (cf. legend "Composite"). Marked is also the gap in the composite profile between 204.719 and 204.804 m c.d., where no overlapping core segments are available. The lithological information includes the classification of the sediments into the three lithotypes (for color code see legend "Lithology"), and information about the water content, TIC, TOC, bSi, TOC/TS, TOC/TN, K, Fe, Zr/K, and grain size variability (< 4 µm grain size fraction). High-resolution XRF data was filtered by using a lowpass filter (5th order, cut off frequency: 0.064 Hz) in order to remove white noise from the data. Red dots mark the results of the conventional XRF analyses. The occurrence of siderite layer, tephra layers, and Mass Movement Deposits (MMD) are indicated on the right column (cf. legend "Lithology"). Tephra layer and Mass Movement Deposits marked with an asterisk are shown in Fig. 3: *1: 1F-4H-3, *2: 1D-24H-2, *3: 1C-68-2, *4: 1F-6H-2, *5: 1D-18H-3.

BGD
12, 15111–15156, 2015

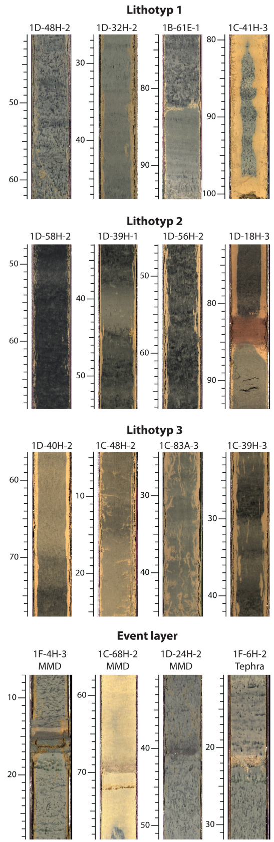

Figure 3. High-resolution line-scan images showing characteristic core segments from deposits of lithotype 1 to 3, and of Mass Movement Deposits (MMD) and tephra layers. The vertical scale is in centimeter section depth.

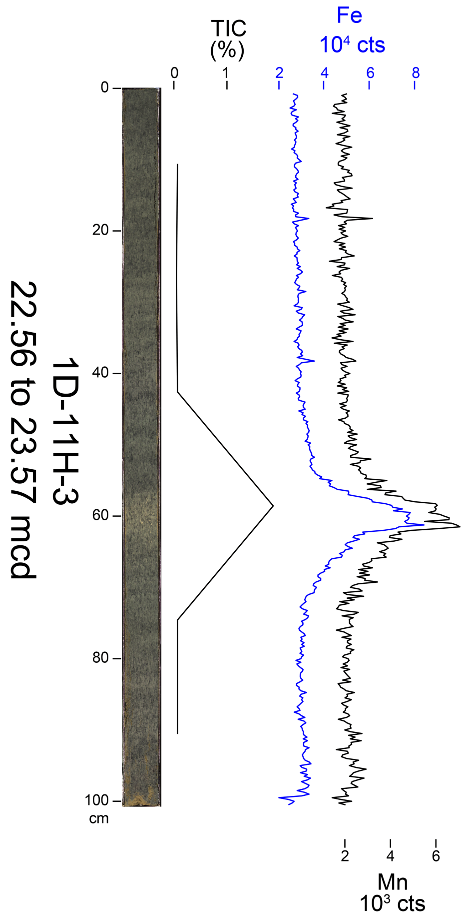

Figure 4. Siderite layer in core 1F-11H-3 (ca. 60 cm section depth) at 22.56 to 23.57 m c.d.. The yellowish brown siderite layer correlates to enhanced TIC, iron (Fe), and manganese (Mn) intensities in the sediments.

BGD
12, 15111–15156, 2015

Title Page
Abstract | Introduction
Conclusions | References
Tables | Figures
◀| |▶
◀ ▶
Back | Close
Full Screen / Esc
Printer-friendly Version
Interactive Discussion

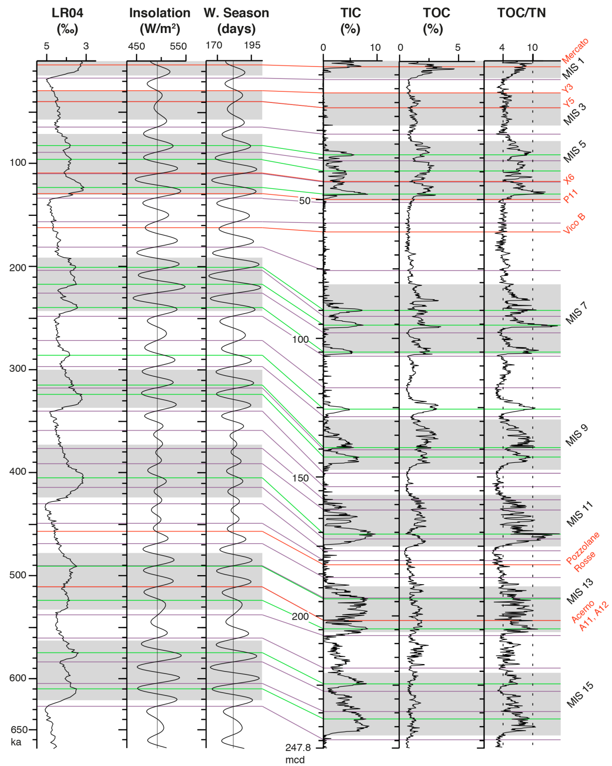

Figure 5. Age modeling of the DEEP site sequence down to 247.8 m c.d., with ages and occurrence of tephra layers (1st order tie points, red), and tuning of TOC and TOC/TN (2nd order tie points, purple) vs. local insolation and winter season length (Laskar et al., 2004), and TIC (3rd order tie points, green) vs. the global benthic isotope stack LR04 and marine isotope stages (MIS, grey) 15 to 1 (Lisiecki and Raymo, 2005).

BGD
12, 15111–15156, 2015

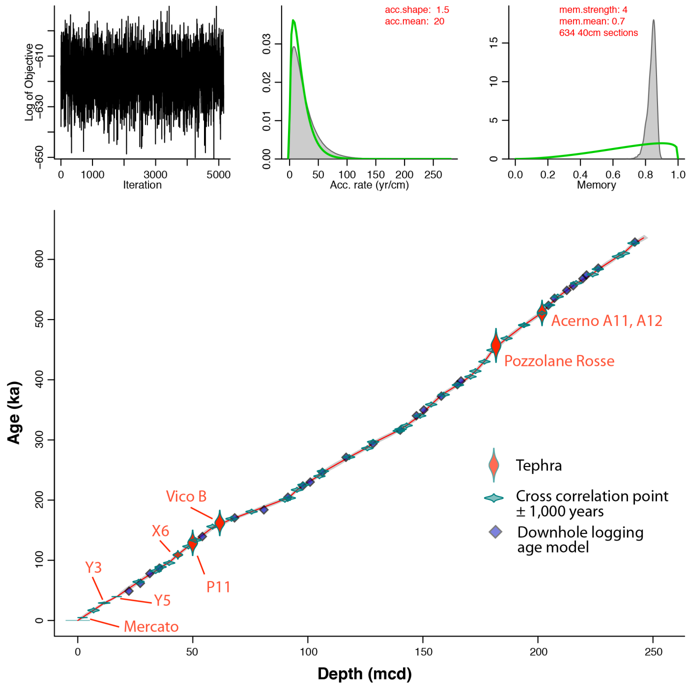

Figure 6. Age model of the DEEP site sequence down to 247.8 m c.d. (640 ka), using the software package Bacon 2.2 (Blaauw and Christen, 2011). Overall stable sedimentation rates at the DEEP site (mem.strength = 4, mem.shape = 0.7, thick = 40 cm) and expected sedimentation rates (acc.shape = 1.5, acc.mean = 20) from first age estimations for the DEEP site sequence by Wagner et al. (2014, cf. Fig. 6) were considered. For the ages and errors of the tephra layers (red) see Table 2. The cross correlation points (green) include an error of ±1000 years. The age model was re-evaluated and refined by a comparison to the age model of the downhole logging data (purple) by Baumgarten et al. (2015).

BGD
12, 15111–15156, 2015

Sedimentological processes and environmental variability at Lake Ohrid

A. Francke et al.

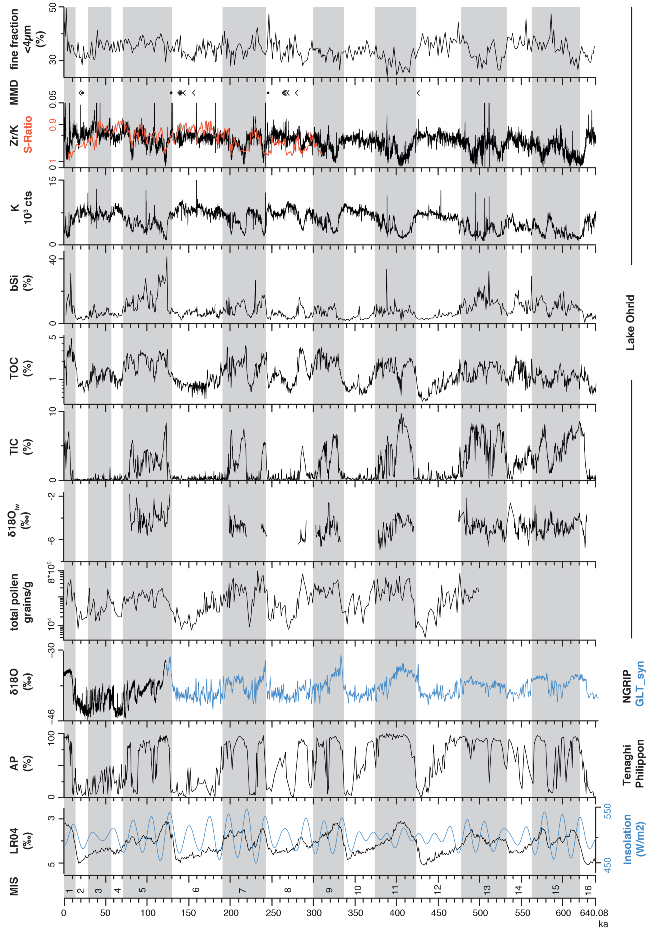

BGD

12, 15111–15156, 2015

Sedimentological processes and environmental variability at Lake Ohrid

A. Francke et al.

Title Page
Abstract | Introduction
Conclusions | References
Tables | Figures
◀| |▶
◀ ▶
Back | Close
Full Screen / Esc
Printer-friendly Version
Interactive Discussion

Figure 7. Proxy data from the DEEP site sequence plotted vs. age and compared to the global benthic isotope stack LR04 (Lisiecki and Raymo, 2005), the local (41° N) insolation at 21 June, the arboreal pollen concentration (AP) in the Tenaghi Philippon record in northern Greece (Tzedakis et al., 2006), the north Greenland temperature derived from the NGRIP $\delta^{18}O$ record (‰ VSMOW, NGRIP-members, 2004) and the GL_T_syn $\delta^{18}O$ synthetic isotope record (‰ VSMOW, Barker et al., 2011). The grey shaded areas indicate interglacial marine isotope stages (MIS; Lisiecki and Raymo, 2005). For the legend of the Mass Movement Deposits (MMD) see Fig. 2. High-resolution XRF data was filtered by using a lowpass filter (5th order, cut off frequency: 0.064 Hz) in order to remove white noise from the data. Note the logarithmic scale for TOC. Pollen concentrations are from Sadori et al. (2015), lake water $\delta^{18}O_{lw}$ from Lacey et al. (2015), and *S* ratios representing hematite + goethite vs. magnetite from Just et al. (2015).

BGD
12, 15111–15156, 2015

Sedimentological processes and environmental variability at Lake Ohrid

A. Francke et al.